Endocrine Glands

6

Tao Huang and Xin Jing

Thyroid Gland

The thyroid is a vascular-rich, butterfly-shaped organ located at the base of the anterior neck that lies on the anterolateral aspect of the cervical trachea, just covering the thyroid cartilage and adjacent tracheal rings. It consists of a left and right lobe, connected by a typically thin isthmus. In adults, the thyroid gland usually weighs 15–25 g, although there can be variation between individuals of different gender, age, weight, and hormonal status as well as exposure to various environmental factors. Each lobe measures approximately 4 cm in length, 2 cm in width, and 2–3 cm in thickness. The isthmus measures approximately 2 cm in length and 2 cm in height, but can have a width that ranges from 2 to 6 cm. It is not uncommon for a normal thyroid lobe to contain an additional thin pyramidal lobe extending superiorly from the isthmus as a remnant of the thyroglossal duct. A small proportion of normal thyroid glands can have nodularity. The thyroid's main function is the production of hormones, the most important of which are thyroxine (T4) and biologically active triiodothyronine (T3) that exert metabolic effects throughout end-organ targets. T4 and approximately 20% of T3 are synthesized by the thyroid. However, the majority of T3 is generated from the conversion of T4 to T3 in extrathyroidal peripheral tissues. These thyroid hormones participate in the regulation of metabolism and growth [1, 2].

On histology, normal thyroid parenchyma is divided into multiple lobules, with each lobule composed of 20–40 various-sized follicles. Follicles have round lumens that are filled with homogeneous eosinophilic colloid, a thick, proteinaceous substance containing thyroglobulin, which serves as a storage point for inactive thyroid hormone precursors and iodine as well as a substrate for the synthesis of thyroid hormones. The follicles are lined by a single layer of flat, cuboidal, or low columnar follicular epithelial cells that display round to ovoid nuclei and fine granular to clumped chromatin. Thyroid follicular cells are responsible for the synthesis of the T4 and T3 hormones and thyroglobulin. The amount of cytoplasm within the follicular cells varies depending on their degree of activity. Flat follicular cells are inactive (Fig. 6.1a), whereas cuboidal cells synthesize thyroglobulin and other proteins to be subsequently stored in luminal colloid. Low columnar cells actively absorb colloid and are therefore often associated with absorption vacuoles (Fig. 6.1b). Calcium oxalate crystals are often present within the colloid material and this finding is thought to be associated with a low functional status of thyroid follicles (Fig. 6.1c) [3]. The shape of these crystals varies and they can be easily detected with polarization. The identification of calcium oxalate crystals within thyroid is helpful during frozen sections in separating thyroid from parathyroid tissue. Follicular cells may show features of Hürthle cell metaplasia manifested by abundant finely granular cytoplasm, a round nucleus, and a variably conspicuous nucleolus (Fig. 6.1d). Sometimes the normal thyroid gland may contain granulomas that originate from ruptured follicles due to palpation. Lymphocytes may be seen in normal thyroid tissue when in close proximity to a lesion or in sampling of an intrathyroidal lymph node [4]. Cytologic samples of the thyroid may also display other elements, such as fragments of skeletal muscle, dystrophic calcification in elderly persons, intrathyroidal parathyroid tissue, ectopic thymic tissue, ectopic cartilage, and adipose tissue as a result of stromal metaplasia.

Additionally, the thyroid contains calcitonin-producing parafollicular or C cells, which are commonly located in the mid- and upper 1/3 of the lateral lobes and comprise less than 0.1% of the total glandular component of the thyroid. In the normal thyroid, C cells are often inconspicuous, and rarely are appreciated under light microscopic examination of hematoxylin & eosin (H & E)-stained sections [5, 6]. C cells show nuclei which are larger than that of the follicular cells, have finely dispersed nuclear chromatin, inconspicuous nucleoli, and variable amounts of pale to eosinophilic granular cytoplasm (Fig. 6.1e). It is noteworthy to mention that the

T. Huang · X. Jing (✉)
Department of Pathology, University of Michigan, Ann Arbor, MI, USA
e-mail: taohuang@med.umich.edu; xinjing@med.umich.edu

M. Lew et al. (eds.), *Normal Cytology*, https://doi.org/10.1007/978-3-031-20336-7_6

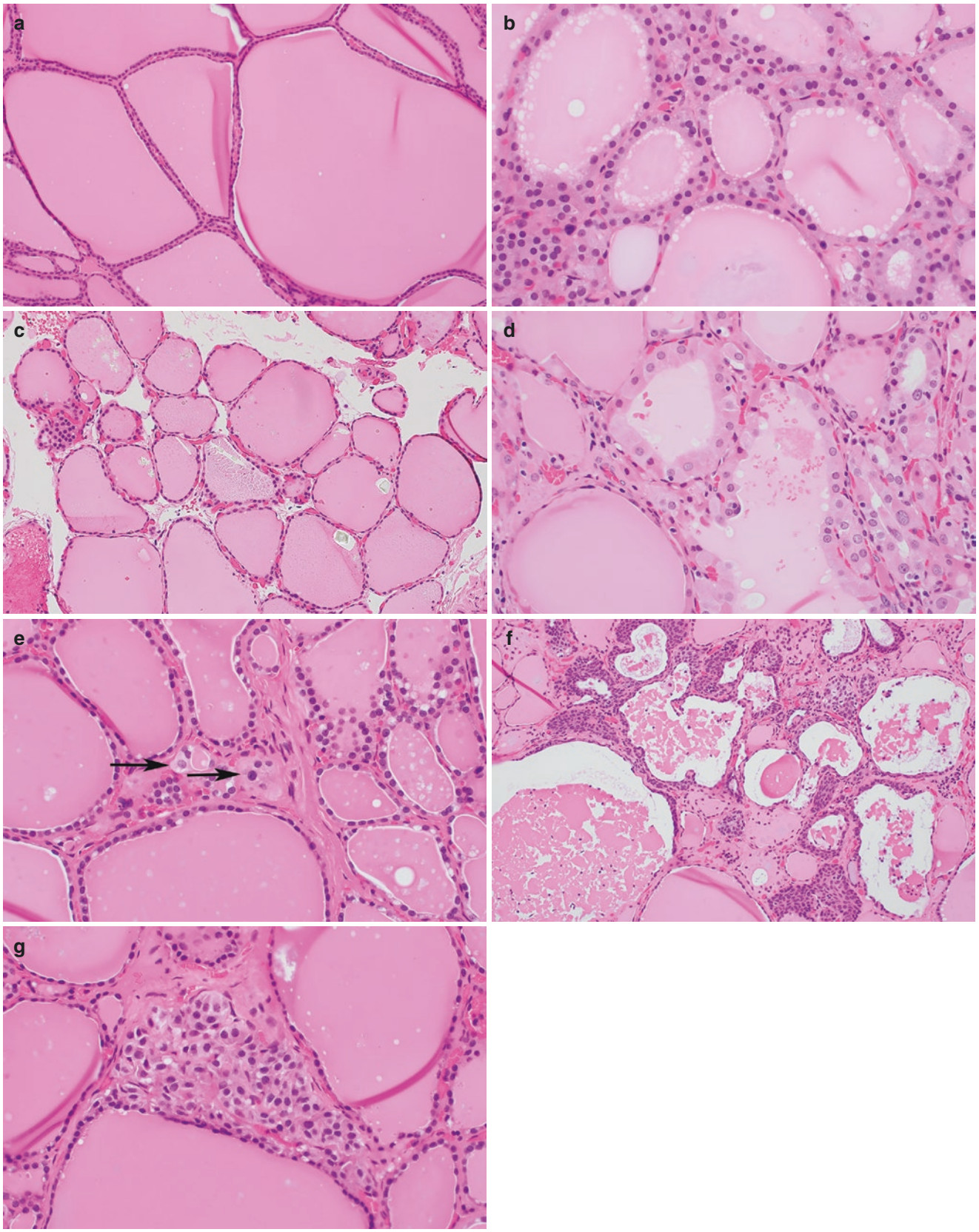

Fig. 6.1 (**a**) Thyroid parenchyma showing variably sized follicles lined by a single layer of flat, inactive, follicular cells (**b**) and/or low columnar cells with absorption vacuoles, filled with (**c**) homogenous eosinophilic colloid with calcium oxalate crystals. (**d**) Metaplastic Hürthle cells with abundant eosinophilic granular cytoplasm can be identified within thyroid parenchyma. (**e**) Parafollicular or C cells can be identified as single cells or as nests of cells (black arrows). (**f**) Small clusters of C cells are readily noted within solid cell nests. (**g**) C cell hyperplasia around a follicle. Thyroid resection, hematoxylin & eosin, 10× (**a**), 20× (**c**), and 40× (**b**, **d**–**g**) magnification

lateral portion of the thyroid lobes may contain solid cell nests, which represent ultimobranchial body remnants derived from the fourth and fifth branchial pouches. Solid cell nests measure from 0.1 to 2 mm and are composed of predominantly basaloid cells and small clusters of C cells (Fig. 6.1f). C cells are more readily identified in abnormal situations, such as C cell hyperplasia in patients with multiple endocrine neoplasia type 2 (Fig. 6.1g). The immunohistochemical stains of calcitonin and neuroendocrine markers including synaptophysin and chromogranin can be used to identify C cells.

Ultrasound is considered the best imaging modality for comprehensive evaluation of the thyroid. Normal thyroid has a homogeneous appearance, and no internal anatomic landmarks are typically defined upon ultrasound exam [7, 8]. Ultrasound-guided fine needle aspiration (FNA) is utilized as an important tool in the clinical assessment and management of thyroid nodules [9]. The anatomy of the thyroid gland on ultrasound imaging and neighboring structures in the neck, such as large vessels, has become increasingly important for cytopathologists to be aware of now that they are performing more ultrasound-guided FNAs of thyroid nodules. Depending on the clinical presentation and laboratory settings, thyroid FNA specimens may be processed as Diff-Quik and/or Papanicolaou-stained conventional smears and/or liquid-based preparations (LBP) [10], which may or may not be accompanied by H & E-stained cell block preparations.

There is considerable overlap in cytologic features between normal thyroid and benign follicular nodules. Occasionally, distinguishing normal from abnormal findings may be problematic. FNA smears of normal thyroid may reveal a mixture of follicular cells and colloid. Background colloid has two main morphologic appearances—thick or thin/watery, both of which display a homogenous texture and appear pale to dark blue or purple with Diff-Quik staining and pink or pale gray with Papanicolaou staining. Colloid may display cracks on Diff-Quik-stained smears as a result of drying and subsequent retraction of colloid from the slide (Fig. 6.2).

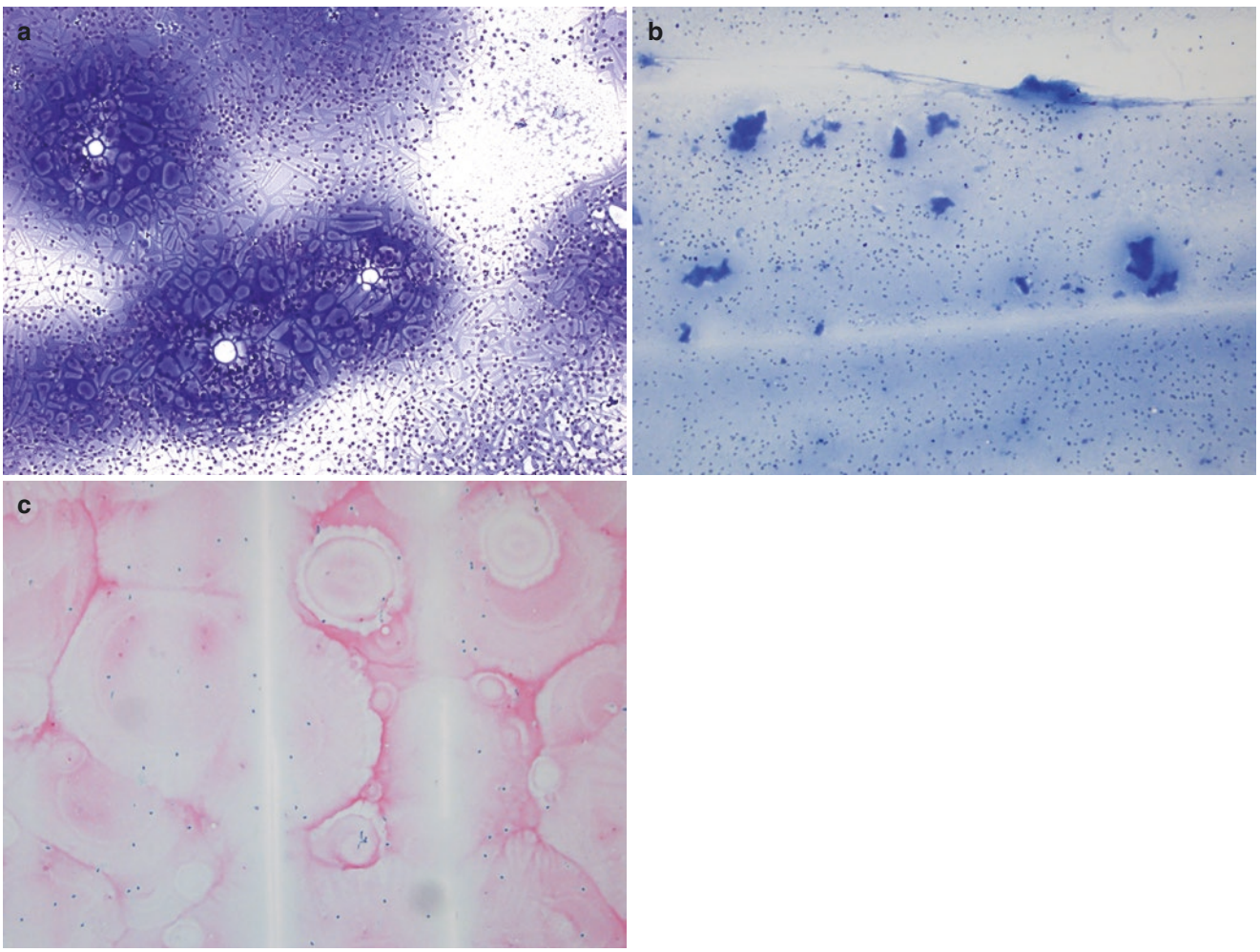

Fig. 6.2 (**a**) Homogenous-appearing thick and thin/watery colloid. Colloid appears blue to purple with Diff-Quik staining and may have cracks as a result of drying and retraction of colloid from the slide. (**b**, **c**) Colloid appears pink or pale gray with Papanicolaou staining. Thyroid, air-dried smear preparation, Diff-Quik, 10× magnification (**a**, **b**). Thyroid, alcohol-fixed smear preparation, Papanicolaou stain, 10× magnification (**c**)

Occasionally smear preparations may show calcium oxalate crystals interspersed with colloid [11, 12]. One should avoid misinterpretation of amyloid and psammomatous calcifications as colloid, which could delay treatment for other disease entities, such as medullary thyroid carcinoma and papillary thyroid carcinoma. Unlike thick and thin colloid material, both of which have homogenous appearance, amyloid material commonly has a coarse, granular texture and is interspersed with elongated and/or spindle-shaped, fibroblast nuclei (Fig. 6.3). Psammoma bodies often show laminated structures.

The majority of follicular cells may be arranged as monolayered honeycomb-like sheets, clusters of loosely arranged macrofollicles with minimal nuclear overlap, and sometimes occasional intact smaller follicles, as well as rare single cells and bare nuclei. In cases where follicular cells are largely stripped of their cytoplasm, the appearance may be similar to that of dispersed lymphocytes. When intact, follicular cells often have a moderate amount of pale, delicate cytoplasm, a centrally located round or oval nucleus, fine chromatin distribution, and inconspicuous or small nucleoli (Figs. 6.4, 6.5, 6.6, and 6.7). Although uncommon, smear preparations of normal (benign) thyroid may also show sheets of Hürthle cells or flame cells. The cytologic features of Hürthle cells are similar to those found in histologic evaluation including abundant, finely granular cytoplasm, large nuclei, and variably prominent nucleoli (Fig. 6.8). However, the quantity of Hürthle cells should be low in sampling of normal thyroid parenchyma. Additionally, in contrast to sampling from Hürthle cell neoplasms, there is a spectrum of Hürthle cell change among follicular cells in the background. Flame cells, which can be seen in Graves' disease, are morphologically distinct in Diff-Quik-stained smear preparations and are characterized by peripheral cytoplasmic vacuoles and an abundant amount of cytoplasm with red to pink frayed edges (Fig. 6.9). Although peripheral vacuoles have been associated with thyroid hyperactivity, as in Graves' disease, some studies have pointed out their nonspecific status and/or demonstrated the lack of correlation between vacuoles and level of thyroid function [3, 5, 6, 13–15]. Rarely, thyroid smear preparations may contain respiratory epithelial cells due to incidental deep sampling of epithelium lining the tracheal wall. Appreciation of the cilia attached to these bronchial epithelial cells is helpful to prevent misinterpretation as a lesional finding (Fig. 6.10). However, ciliated cells may also be identified in sampling of thyroglossal duct cysts. As such, clinical and radiologic correlation of the sampled tissue is of utmost importance in appropriately designating the etiology of these ciliated cells. Usually, the aforementioned calcitonin-producing C cells are not identified in FNA smears of normal thyroid tissue.

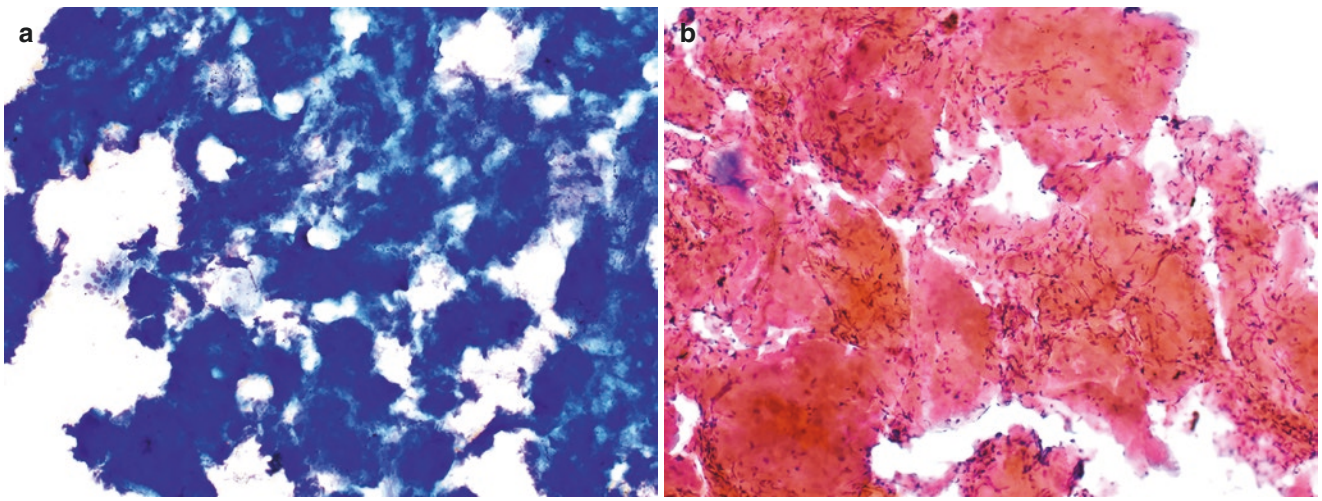

Fig. 6.3 (**a**, **b**) Amyloid material shows a coarse, granular texture that is interspersed with elongated and/or spindle-shaped, fibroblast nuclei. Thyroid, air-dried smear preparation, Diff-Quik, 20× magnification (**a**). Thyroid, alcohol-fixed smear preparation, Papanicolaou stain, 20× magnification (**b**)

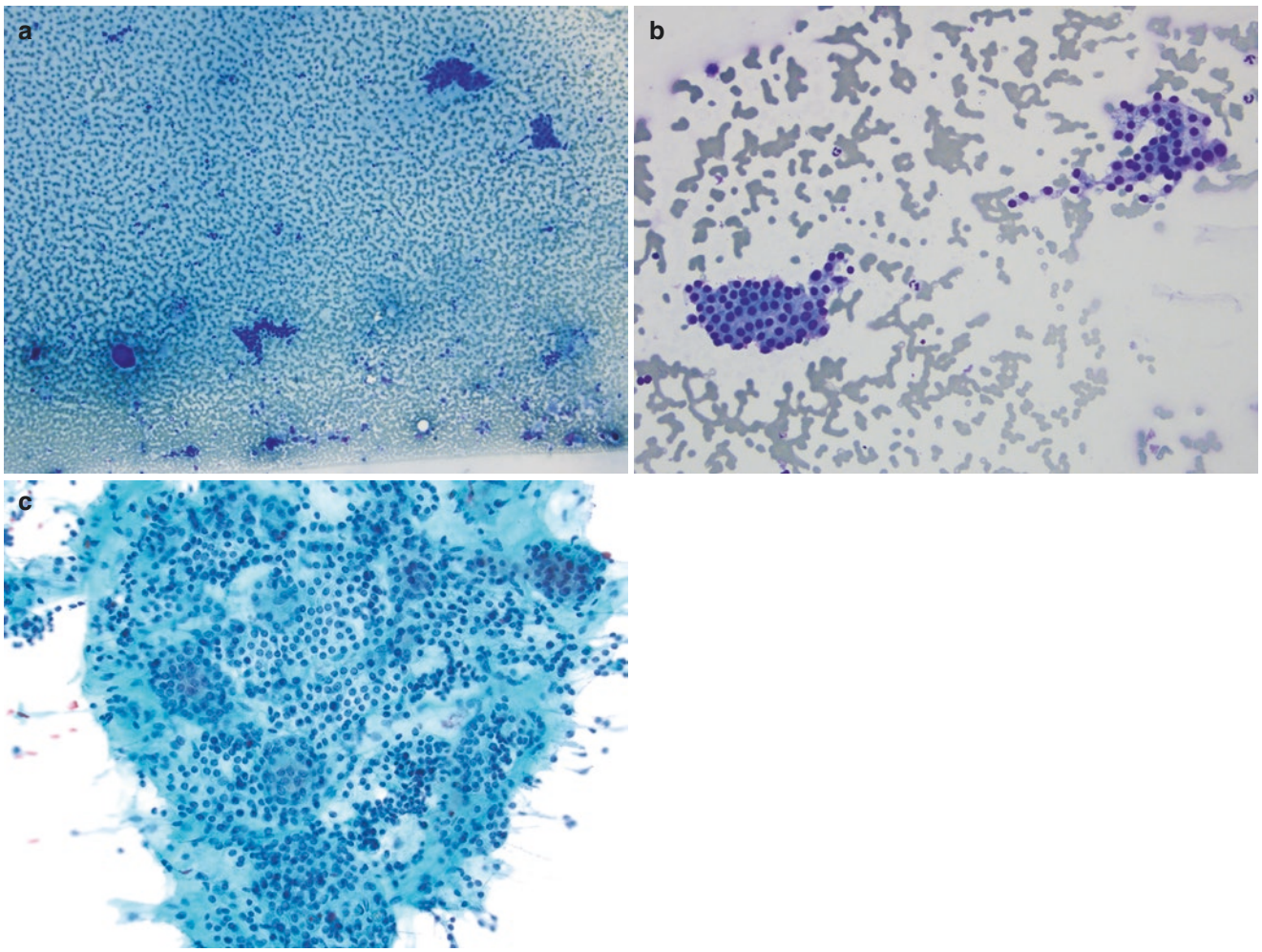

Fig. 6.4 (**a–c**) Background colloid and bland-appearing benign follicular cells which are cohesively arranged in monolayered, honeycomb sheets with even cellular spacing. Note the presence of background watery colloid in these smears. Thyroid, air-dried smear preparation, Diff-Quik, 10× (**a**) and 20× (**b**) magnification. Thyroid, alcohol-fixed preparation, Papanicolaou stain, 20× magnification (**c**)

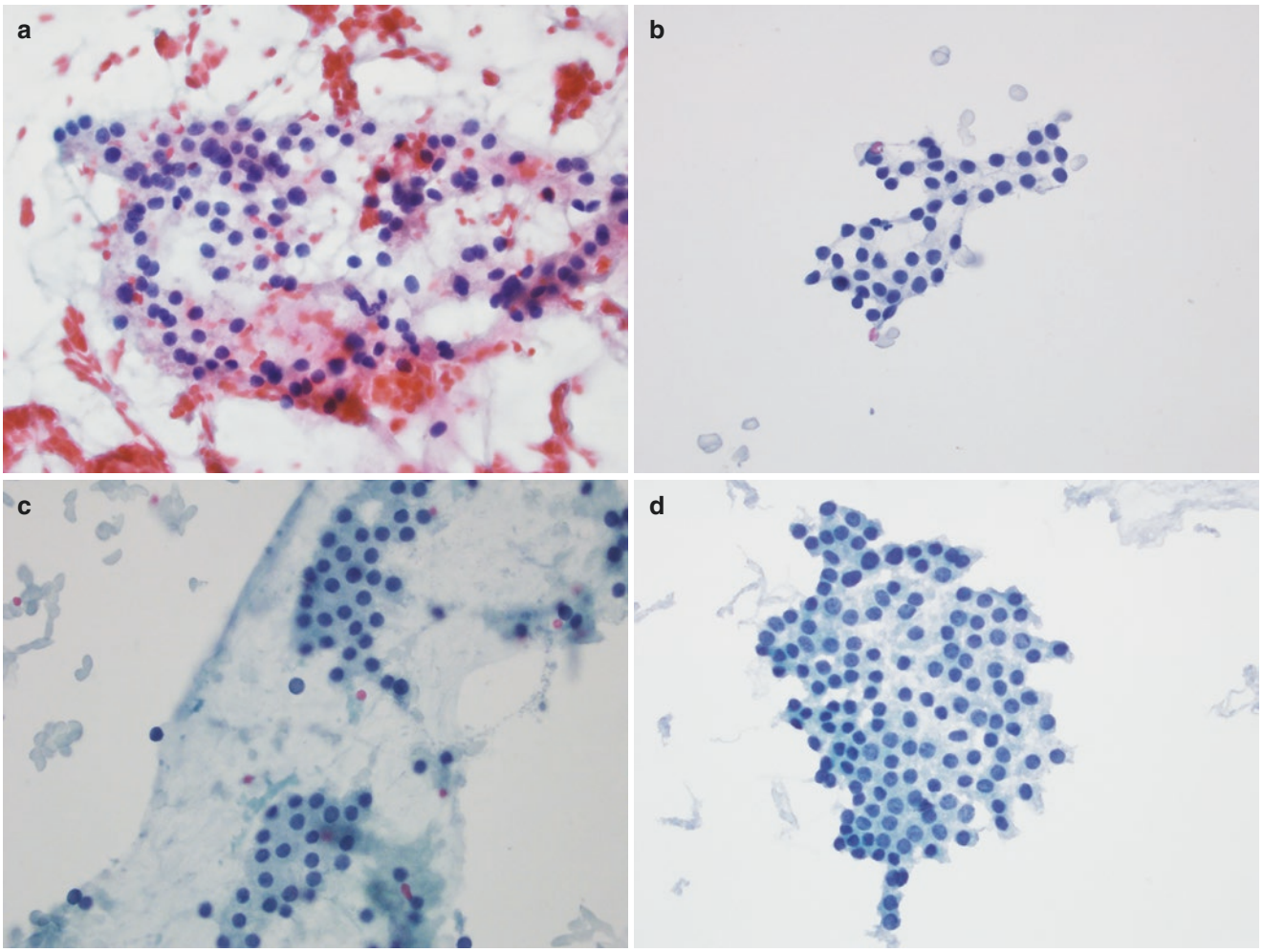

Fig. 6.5 Benign follicular cells arranged as (**a**) a few macrofollicles or (**b**–**d**) monolayered, honeycomb sheets. The follicular cells have a moderate amount of pale cytoplasm, centrally placed round or ovoid nuclei, fine chromatin distribution, and inconspicuous or small nucleoli. Thyroid, alcohol-fixed smear preparation, Papanicolaou stain, 40× magnification (**a**–**c**). Thyroid, ThinPrep preparation, Papanicolaou stain, 40× magnification (**d**)

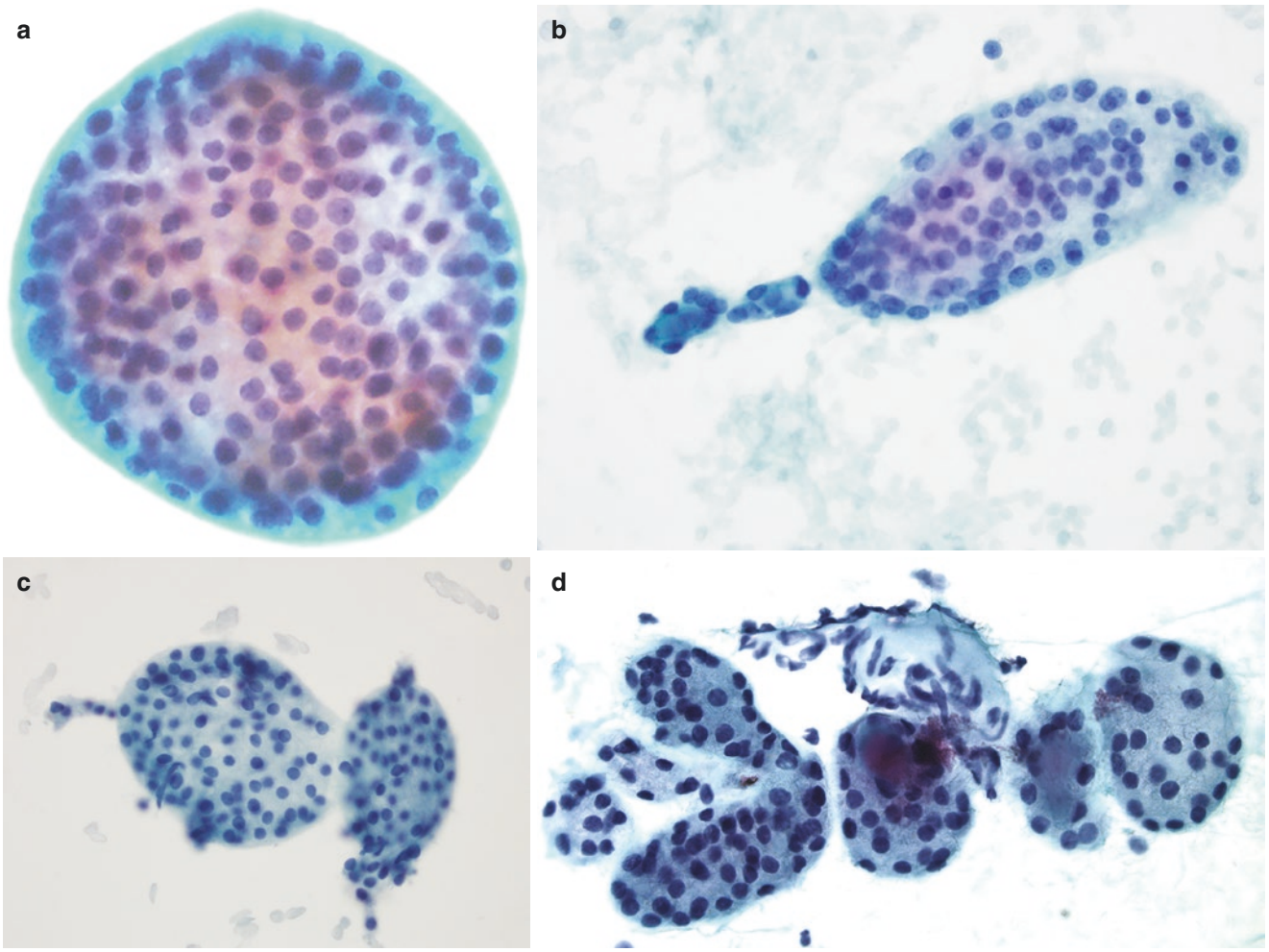

Fig. 6.6 (**a–d**) Benign follicular cells are arranged as intact round follicles which have a smooth outline. The intact follicles may vary in size and contain a few or numerous follicular cells without nuclear overlapping/crowding. Thyroid, alcohol-fixed smear preparation, Papanicolaou stain, 40× magnification (**a–d**)

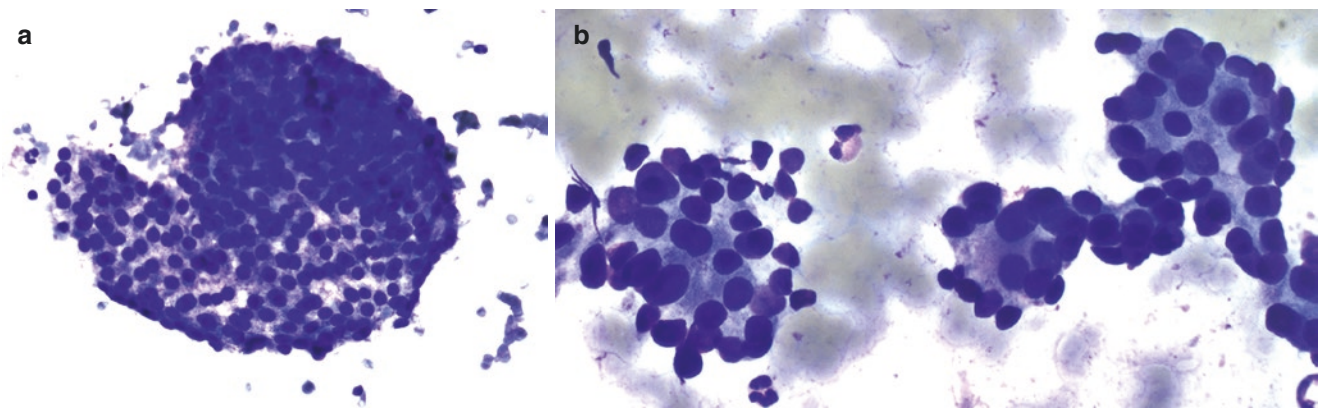

Fig. 6.7 Comparison between (**a**) an intact follicle and (**b**) several smaller microfollicles. Unlike microfollicles, which are defined as crowded cell clusters composed of more than ten follicular cells with significant nuclear overlapping, the intact follicle shows a smooth outline, contains numerous follicular cells in a honeycomb arrangement, and lacks overt nuclear crowding/overlapping. Thyroid, air-dried smear preparation, Diff-Quik, 40× (**a**) and 60× (**b**) magnification

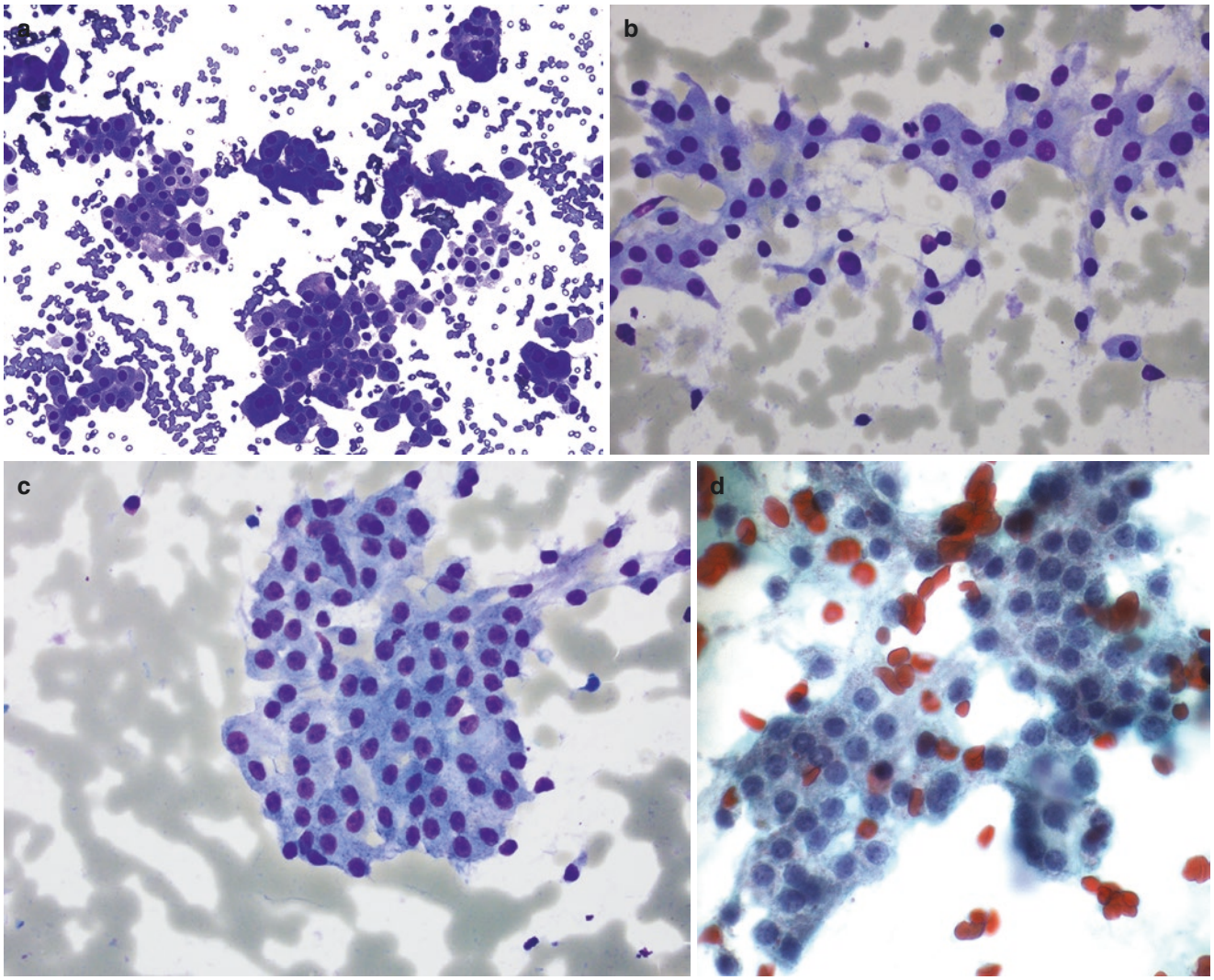

Fig. 6.8 (**a–d**) Singly dispersed and sheets of Hürthle cells with abundant, finely granular cytoplasm, large nuclei, and prominent nucleoli. Thyroid, air-dried smear preparation, Diff-Quik, 20× (**a**) and 40× (**b**, **c**) magnification. Thyroid, alcohol-fixed smear preparation, Papanicolaou stain, 60× magnification (**d**)

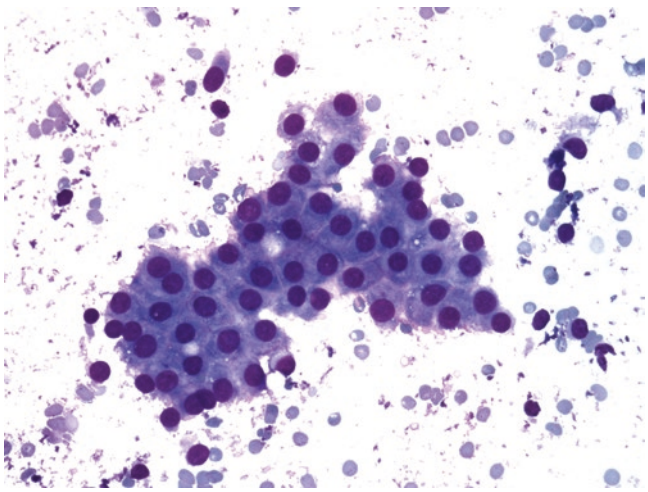

Fig. 6.9 Flame cells have abundant cytoplasm, marginal cytoplasmic vacuoles, and red to pink frayed edges. Thyroid, air-dried smear preparation, Diff-Quik, 40× magnification

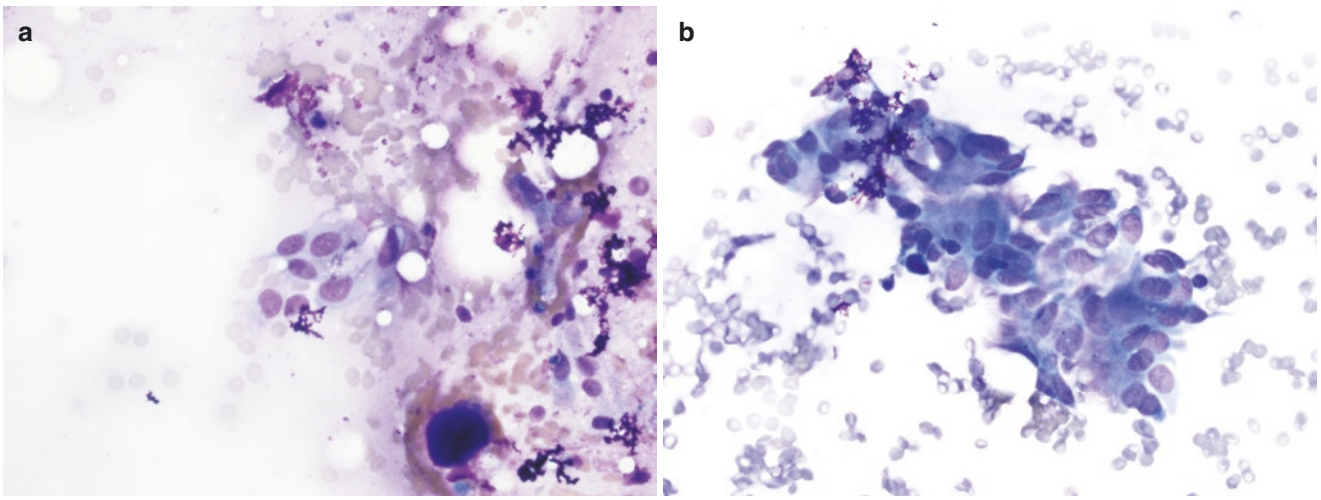

Fig. 6.10 (**a**, **b**) Ciliated respiratory epithelial cells due to contamination from FNA sampling of the trachea. Note the scant dense colloid material in the lower right field of (**a**). Thyroid, air-dried smear preparation, Diff-Quik, 40× magnification (**a, b**)

Parathyroid Glands

Typically, parathyroid glands are present as two paired glands that are located posterior to the upper and lower poles of the thyroid gland. The inferior parathyroid glands may be located anywhere from the level of mandibular angle to pericardium, and the anterior mediastinum is the most common location of finding an ectopic inferior parathyroid gland. Each gland weighs approximately 35–40 mg and measures 0.3–0.8 cm in all three dimensions. Variation in number and location of parathyroids is well described. In this regard, a large autopsy series reported up to 11 glands in normal subjects [1]. Parathyroid glands are responsible for producing parathyroid hormone, which regulates calcium metabolism.

On histology, the parathyroid glands are surrounded by a thin connective tissue capsule and contain a variable amount of adipose tissue within their supporting stroma (Fig. 6.11a, b). This adipose tissue appears after puberty and its amount varies depending on an individual's age and overall functional status of the gland. The average percentage of stromal fat in adult parathyroid glands ranges from 20 to 40% of the entire gland's volume [16, 17]. The parenchyma is rich in vasculature with abundant capillaries surrounding chief cells within lobules (Fig. 6.11c). The chief cells are the predominant cellular element of parathyroid parenchyma, and are characterized by uniform, centrally located, round, and hyperchromatic nuclei, inconspicuous nucleoli, well-defined cell boundaries, and abundant pale-staining to eosinophilic cytoplasm with a variable amount of glycogen and lipid droplets (Fig. 6.11c). Other types of cells identified in the parathyroid include oxyphil and water clear cells, which are postulated to represent morphologic variations of chief cells [18]. Oxyphil cells are characterized by larger nuclei, variably conspicuous nucleoli, and abundant eosinophilic granular cytoplasm (Fig. 6.11d). Water clear cells are rarely seen in normal parathyroid glands and are characterized by well-demarcated cell boundaries and abundant optically clear cytoplasm as a result of glycogen accumulation (Fig. 6.11e). Occasionally, chief cells form small acinar or glandular structures containing eosinophilic colloid-like material within the lumen, mimicking the appearance of thyroid follicles (Fig. 6.11f). When these follicles form and become abundant, the distinction between parathyroid and thyroid tissue can be challenging especially on frozen sections. As mentioned previously, identification of calcium oxalate crystals within colloid is a helpful morphologic clue to confirm thyroid origin.

Due to their location, small size, and thyroid-like pattern of parenchyma, parathyroid glands are not typically detectable on any imaging modality. Preoperative FNA has been used for locating suspected parathyroid tissue. It has been claimed that cytomorphologic features along with ancillary studies (i.e., immunostaining, chemical analysis of FNA rinses, or molecular testing) may aid in confirming parathyroid origin of sampled cells. However, definitive differentiation between normal parathyroid, parathyroid hyperplasia, and a parathyroid adenoma cannot be made by evaluation of cytomorphologic features alone and requires histologic evaluation [19–21].

FNA samples from normal parathyroid glands contain variable amounts of relatively monotonous small round or ovoid chief cells which can be arranged as single cells, cords, loose two-dimensional sheets, papillary structures, three-dimensional clusters, and occasionally microfollicles (Fig. 6.12a, c). Isolated cells and naked nuclei are commonly present. The majority of the cells have moderately abundant amounts of granular and delicate cytoplasm, round nuclei, granular chromatin distribution, and inconspicuous nucleoli.

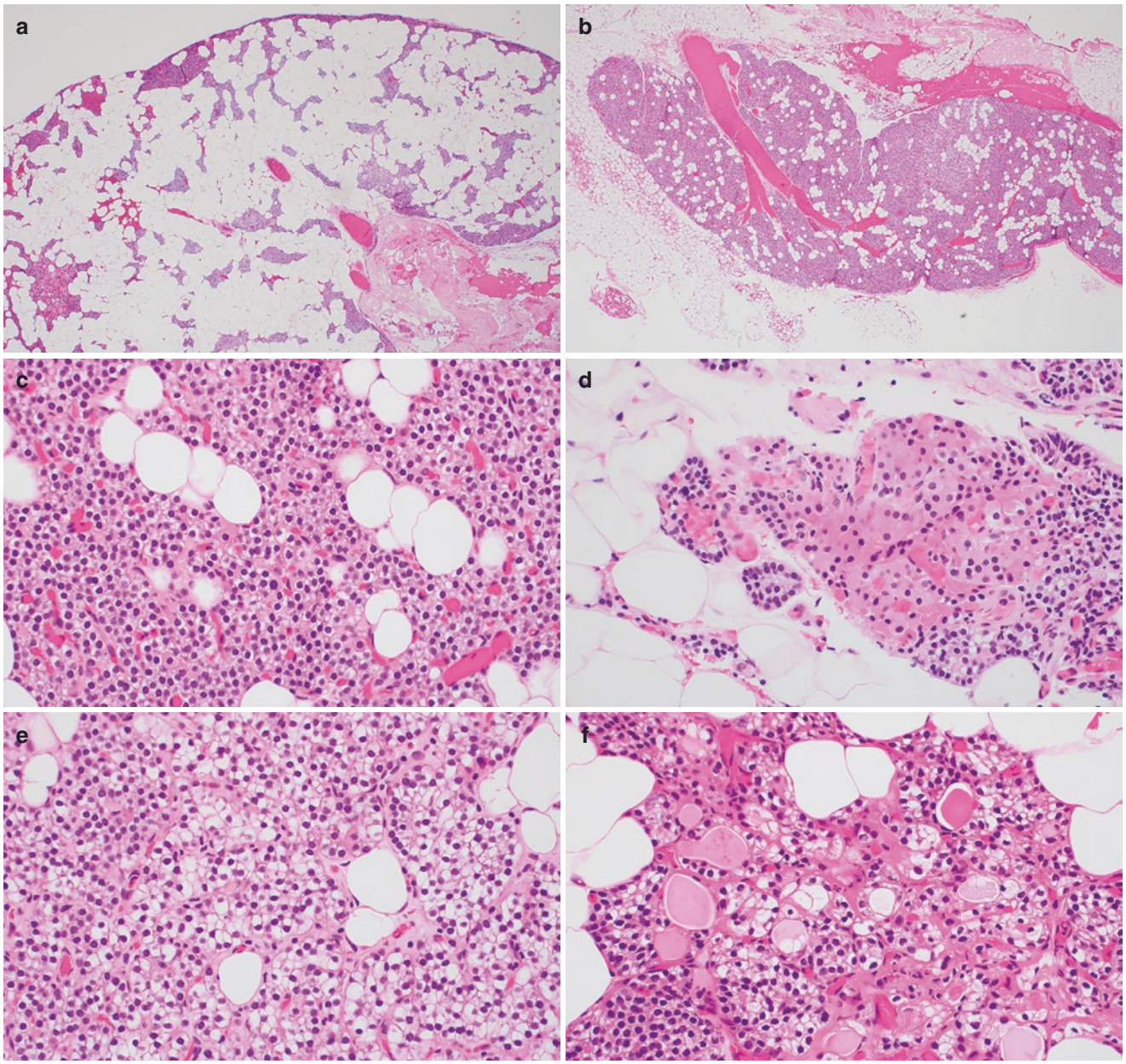

Fig. 6.11 (**a**, **b**) Normal parathyroid glands show a variable amount of stromal fat (**c**) with an extensive delicate capillary network intimately associated with chief cells, (**d**) oxyphil cells, and (**e**) water clear cells. (**f**) Chief cells can occasionally be arranged in acinar or glandular formations with colloid-like material within the lumen mimicking the appearance of thyroid follicles. Parathyroid resection, hematoxylin & eosin, 5× (**a–b**) and 40× (**c–f**) magnification

In addition, a prominent vascular network, mild nuclear pleomorphism, hyperchromatic nuclei, distinct nucleoli, a granular background due to disrupted fragile cytoplasm, and/or colloid-like material may occasionally be present [19–22]. There is considerable overlap in the cytomorphological features of parathyroid and thyroid aspirate samples. However, the presence of stippled chromatin patterns, a vascular network with attached epithelioid cells, and numerous singly dispersed cells and naked nuclei favor a parathyroid origin [19, 20]. Given the significant overlap in cytomorphology, ancillary studies are typically performed to differentiate between these two tissue origins, including chemical analysis of aspirate material (i.e., PTH) and immunohistochemistry on cell block material. PTH will be positive in parathyroid cells (Fig. 6.12h) while thyroid follicular cells are highlighted by PAX-8, TTF-1, and thyroglobulin. Odronic et al. compared the cytomorphological features of parathyroid aspirates between ThinPrep preparations and conventional

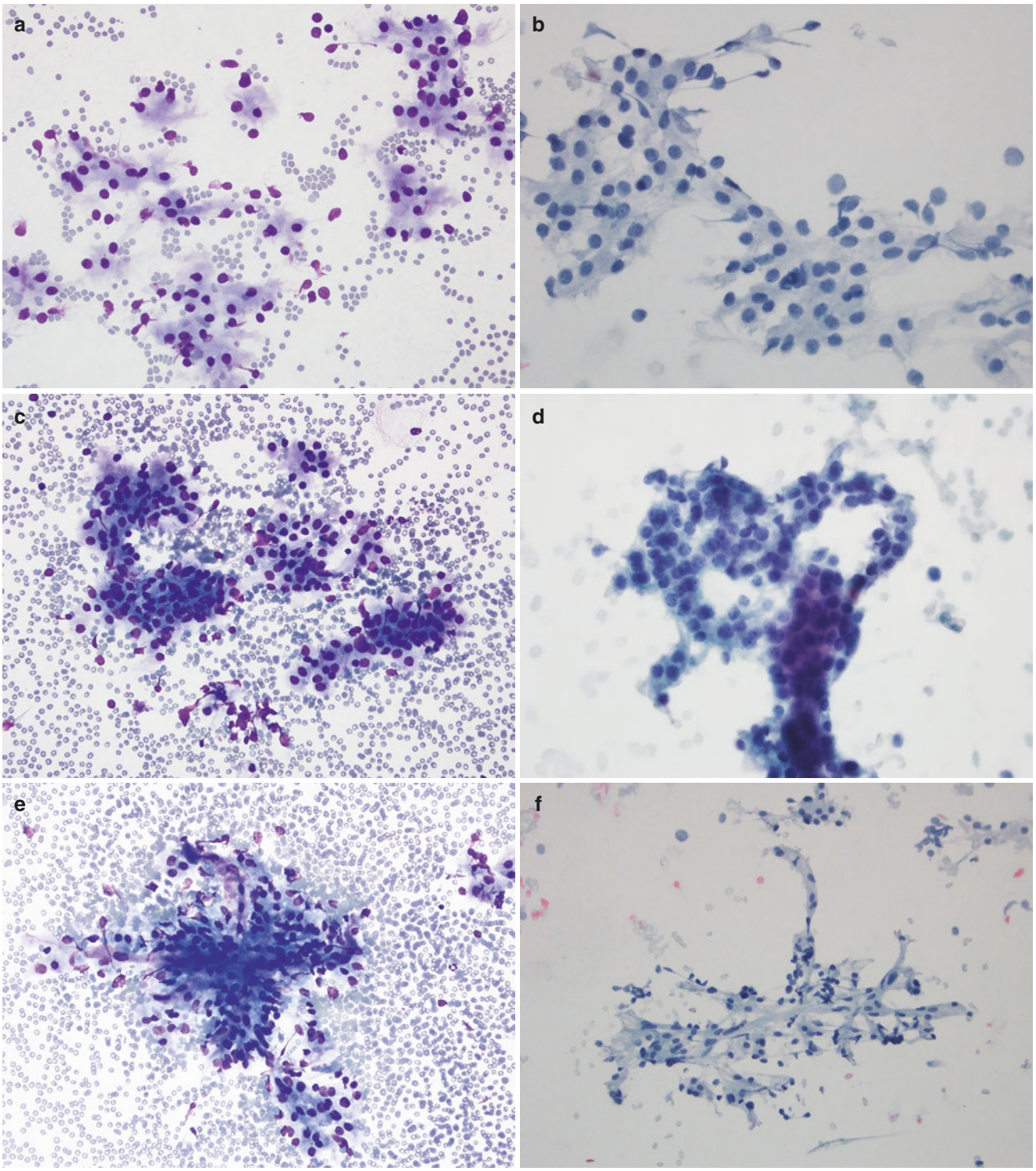

Fig. 6.12 (**a**, **b**) Normal parathyroid cells are arranged as single cells, loose two-dimensional sheets, three-dimensional clusters, and microfollicles. Cells with more abundant granular cytoplasm and prominent nuclei represent oxyphil cells while cells containing relatively smaller amounts of cytoplasm are (**c**, **d**) chief cells. (**e**, **f**) A prominent vascular network and (**g**) colloid-like material may present. (**h**) Positive immunostaining for parathyroid hormone (PTH) can facilitate confirmation of parathyroid cell origin on cell block material. Air-dried smear preparation, Diff-Quik, 20× magnification (**a**, **c**, **e**). Alcohol-fixed smear preparation, Papanicolaou stain, 20× (**f**, **g**) and 40× (**b**, **d**) magnification. Cell block, PTH immunohistochemistry, 10× magnification (**h**)

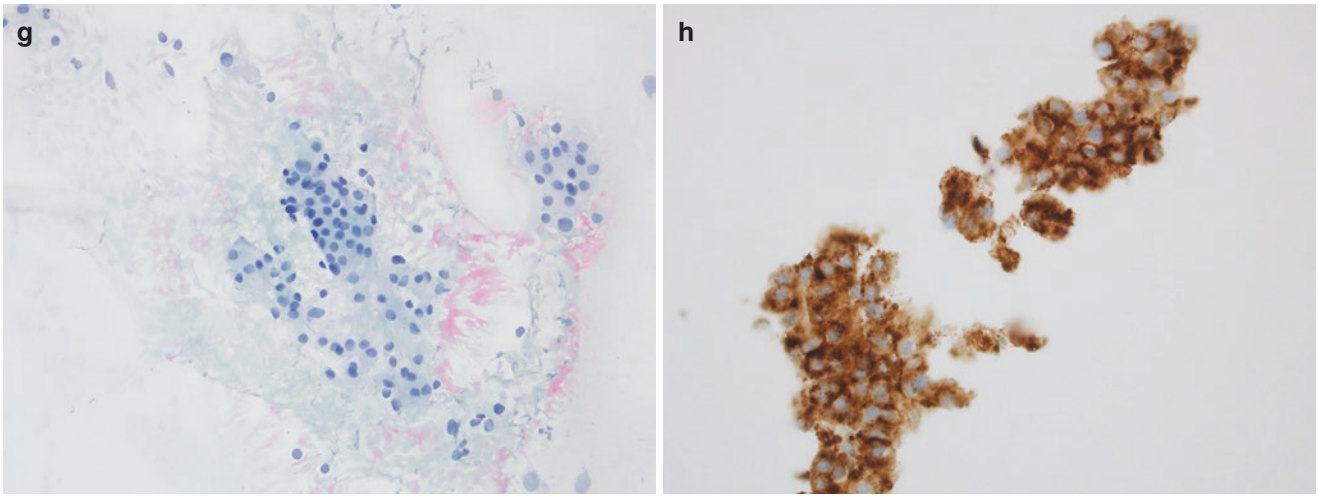

Fig. 6.12 (continued)

smears. Accordingly, ThinPrep preparation did not show papillary architecture and naked nuclei but demonstrated more microfollicles [23, 24].

Adrenal Glands

The right and left adrenal glands are each located superior and medial to the ipsilateral kidney in the retroperitoneum. These glands are composed of a cortex and medulla (Fig. 6.13a). The adrenal cortex is divided into three layers including the outer layer or zona glomerulosa, the middle layer or zona fasciculata, and the inner layer or zona reticularis (Fig. 6.13b). The adrenal cortex secretes several steroid hormones including aldosterone, glucocorticoids, and sex hormones produced by the cortical cells of the zona glomerulosa, zona fasciculata, and zona reticularis, respectively. The zona glomerulosa forms a thin layer and is located directly beneath the fibrous capsule that encompasses the adrenal gland. The cells within zona glomerulosa are arranged in tightly packed small nests with variably scant eosinophilic to amphophilic cytoplasm. In contrast, the adjacent zona fasciculata cells display voluminous finely vacuolated cytoplasm (Fig. 6.13c). The zona fasciculata accounts for the majority of the adrenal cortex and is composed of large cells with vacuolated lipid–rich cytoplasm arranged in two cell-thick cords (Fig. 6.13b, c). The cells of the zona reticularis are large cells with abundant, deeply eosinophilic cytoplasm (Fig. 6.13d). The zona reticularis cells may show prominent golden brown lipofuscin pigment within the cytoplasm (Fig. 6.13e). The central adrenal medulla is mainly composed of large polygonal chromaffin cells with large vesicular nuclei, small nucleoli, and abundant basophilic granular cytoplasm. They are arranged in small nests associated with a delicate capillary network (Fig. 6.13f). Sustentacular cells are located at the periphery of the nests, which are difficult to identify on routine H & E stain, but can be readily highlighted by an S100 immunohistochemical stain.

FNA has been a useful tool in evaluating adrenal lesions including those identified incidentally. In comparison to a percutaneous image-guided approach, endoscopic ultrasound (EUS)-guided FNA is preferred, particularly for the left adrenal gland due to markedly improved specimen adequacy, a less invasive approach, and rare post-procedure complications [25–29]. Normal elements of other viscera may be accidentally sampled in each approach as the needle may traverse other organs to collect adrenal gland samples. Aspirates of the right adrenal gland collected through the percutaneous approach may contain hepatocytes. Similarly, EUS-guided FNAs may contain glandular epithelial cells from the luminal gastrointestinal tract.

The published literature associated with FNA of adrenal glands mainly describes elements of the adrenal cortex. It has been emphasized that cells of the normal adrenal cortex cannot be distinguished from those of adrenal cortical hyperplasia and adenoma merely based on cytomorphological features, as all these three conditions exhibit overlapping cytomorphological findings. Clinical and radiological correlation thus plays an important role for accurate interpretation. FNA smears may show a lipid-rich, bubbly background characterized by small, punched-out, round vacuoles, and single and/or loose clusters of cells. The cells have ill-defined, fragile, vacuolated or foamy cytoplasm, centrally or eccentrically located round nuclei, evenly distributed chromatin, and inconspicuous or distinct nucleoli (Fig. 6.14a–d). Variation in nuclear size may be observed, and should not always be regarded as pleomorphism of neoplasia. In addition, abundant stripped nuclei in the background of large,

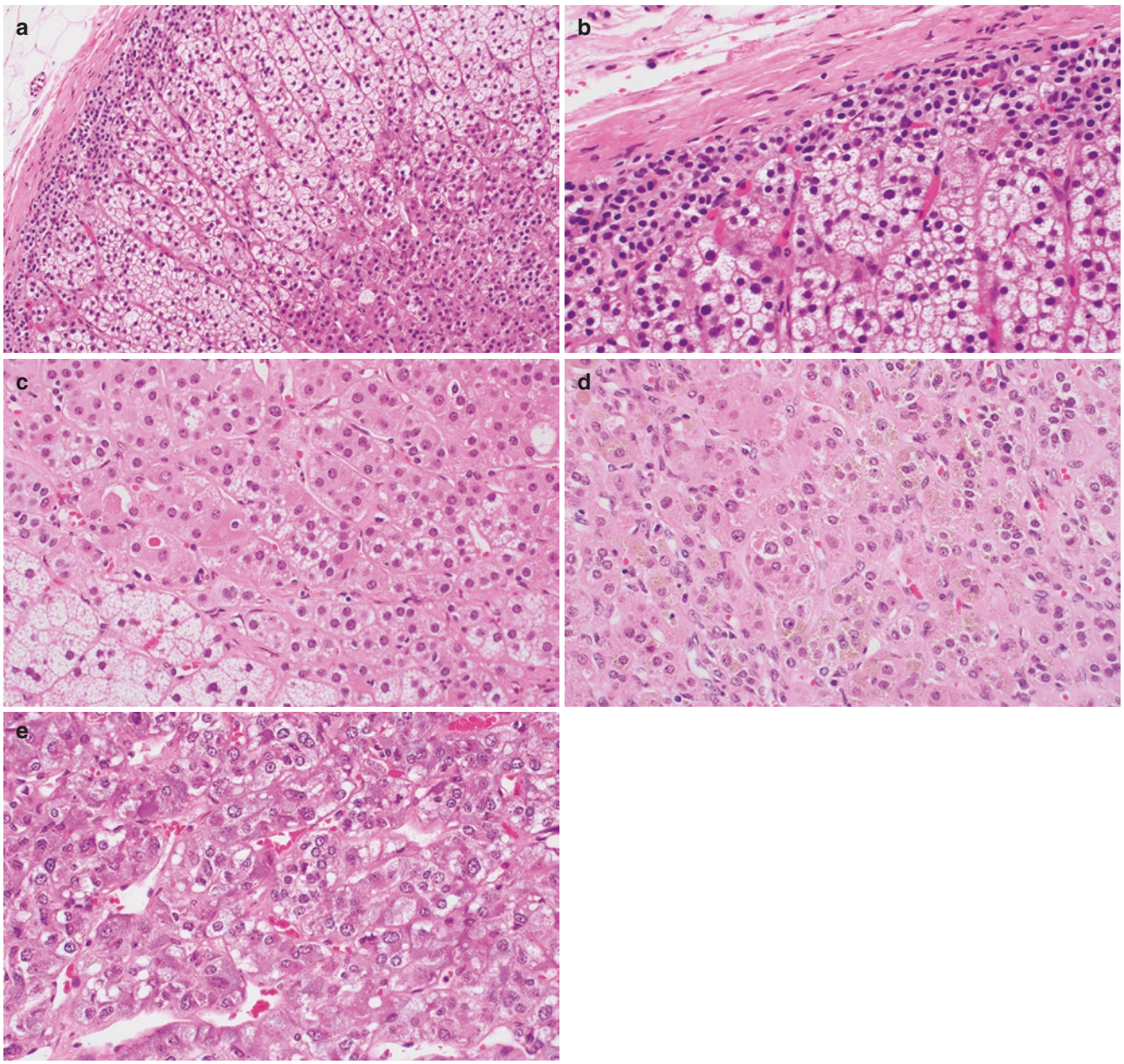

Fig. 6.13 (**a**) The adrenal cortex is composed of three distinct layers including the outermost zona glomerulosa, middle zona fasciculata, and innermost zona reticularis. (**b**) The zona glomerulosa cells are located directly underneath the capsule with scant eosinophilic to amphophilic cytoplasm in contrast to the voluminous finely vacuolated and lipid-rich cytoplasm of the zona fasciculata cells. (**c**) The zona reticularis cells are large with abundant, deeply eosinophilic cytoplasm and (**d**) occasionally display intracytoplasmic golden-brown lipofuscin pigment. (**e**) The adrenal medulla is composed of mainly large polygonal chromaffin cells arranged in small nests. Adrenal gland resection, hematoxylin & eosin, 20× (**a**) and 40× (**b**–**e**) magnification

cohesive tissue fragments composed of adrenal cortical cells (Fig. 6.14e, f) in syncytial and nested arrangements admixed with sinusoidal endothelial cells (Fig. 6.14g, h) are frequently observed. The combination of a lipid-rich, bubbly background along with bare nuclei (Fig. 6.14i–k) and large tissue fragments (Fig. 6.14l) thus favors sampling of benign adrenal gland over metastatic disease (e.g., renal cell carcinoma or hepatocellular carcinoma) [28–30]. A panel of immunohistochemistry with inhibin, PAX-8, Hep-par 1, and arginase performed on cell block material with adequate cellularity may also be helpful in delineating the etiology of cell types. Inhibin will highlight adrenal cortical cells while PAX-8 frequently highlights renal cell carcinoma and Hep-par 1 and arginase highlight hepatocytic cells.

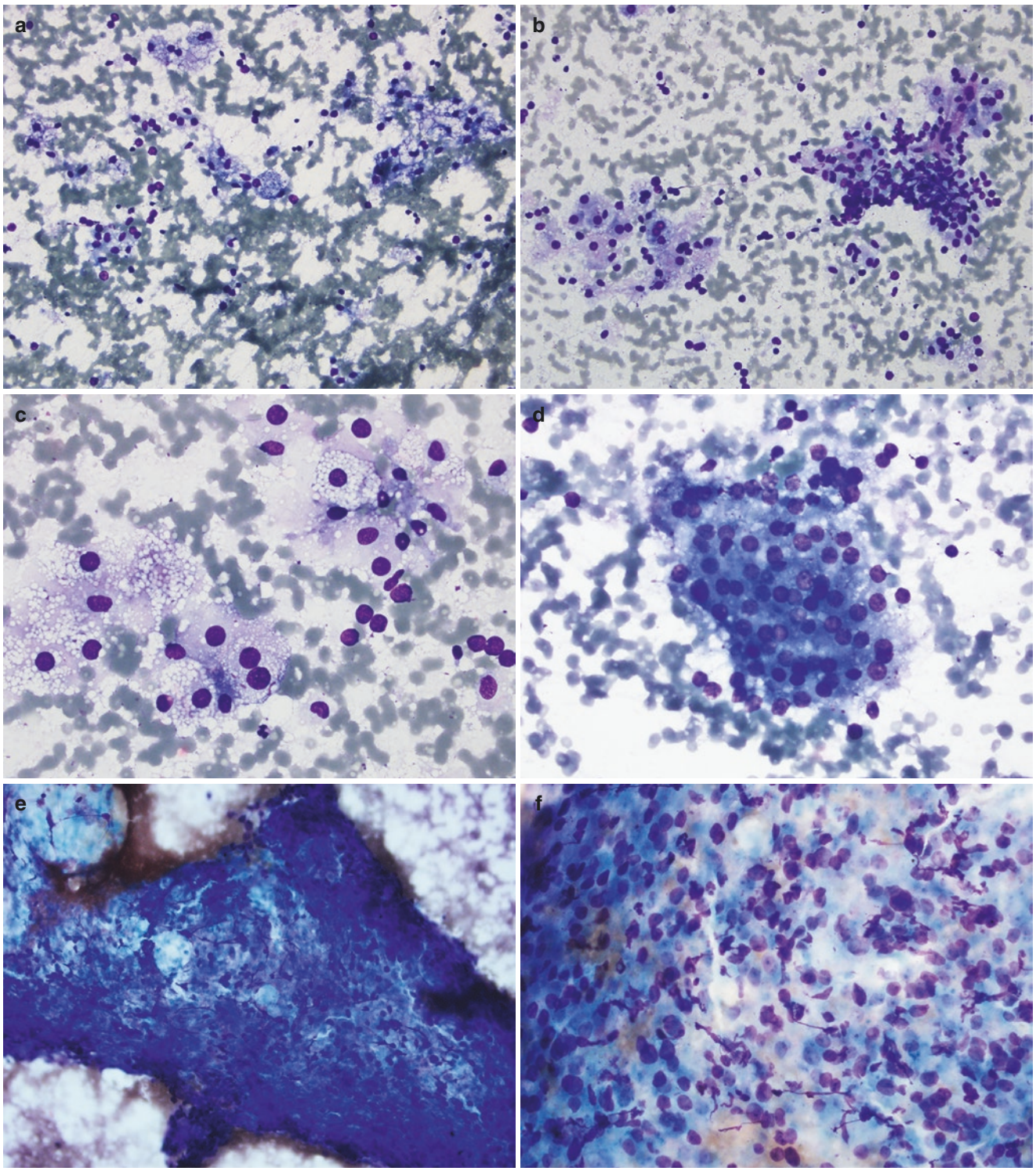

Fig. 6.14 (**a**–**d**) Adrenal cortical cells with ill-defined, vacuolated or foamy cytoplasm, centrally or eccentrically located round nuclei, evenly distributed chromatin, and inconspicuous or distinct nucleoli arranged singly and in loose clusters. (**e**, **f**) Adrenal cortical cells can also be identified in large, cohesive tissue fragments admixed with sinusoidal endothelial cells. (**g**, **h**) Abundant stripped or naked nuclei can also be seen in the background of cortical cells arranged as (**i**–**k**) clusters or (**l**) sheets. Adrenal gland, air-dried smear preparation, Diff-Quik, 20× (**a**, **b**, **e**) and 40× (**c**, **d**, **f**) magnification. Adrenal gland, alcohol-fixed smear preparation, Papanicolaou stain, 20× (**g**, **h**), 40× (**i**, **l**), and 60× (**j**, **k**) magnification

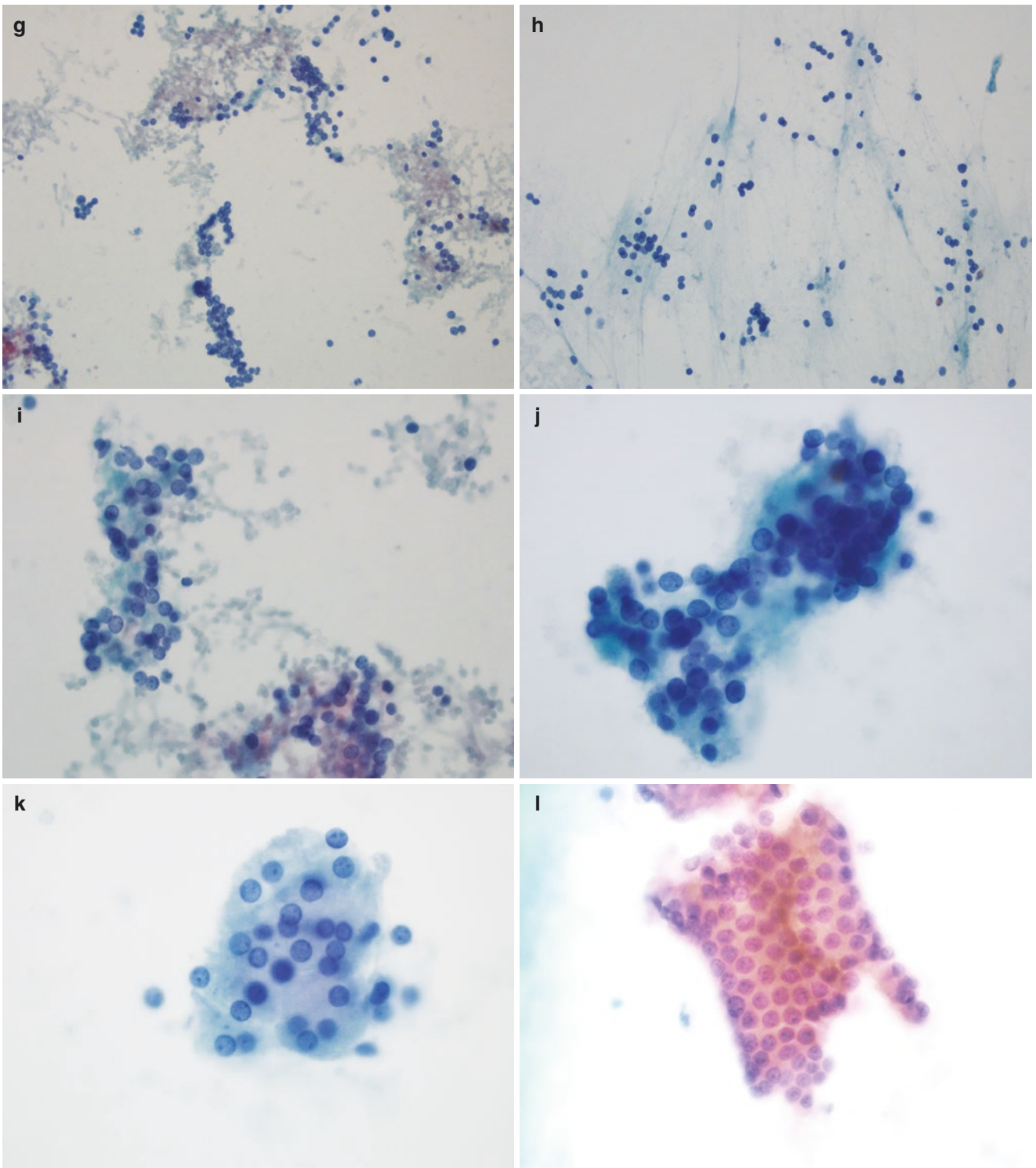

Fig. 6.14 (continued)

References

1. Mohebati A, Shaha AR. Anatomy of thyroid and parathyroid glands and neurovascular relations. Clin Anat. 2012;25(1):19–31.
2. Allen E, Fingeret A. Anatomy, head and neck, thyroid. Treasure Island, FL: StatPearls; 2020.
3. Katoh R, et al. Nature and significance of calcium oxalate crystals in normal human thyroid gland. A clinicopathological and immunohistochemical study. Virchows Arch A Pathol Anat Histopathol. 1993;422(4):301–6.
4. Shawky MS, Meyer-Rochow W. Aberrant intrathyroid tissue: a report of intrathyroid lymph node metastasis and a review of literature. Indian J Surg. 2017;79(2):148–52.
5. Herzberg AJ, Raso DS, Silverman JF. Thyroid. In: Herzberg AJ, Raso DS, Silverman JF, editors. Color atlas of normal cytology. Philadelphia: Churchill Livingstone; 1999. p. 197–8.
6. Galera-Davidson H, González-Cámpora R. Thyroid. In: Bibbo M, Wilbur D, editors. Comprehensive cytopathology. Philadelphia: Saunders Elsevier; 2008. p. 636.
7. Germano A, et al. Normal ultrasound anatomy and common anatomical variants of the thyroid gland plus adjacent structures—a pictorial review. Clin Imaging. 2019;58:114–28.
8. Richman DM, Frates MC. Ultrasound of the normal thyroid with technical pearls and pitfalls. Radiol Clin North Am. 2020;58(6):1033–9.
9. Haugen BR, et al. 2015 American Thyroid Association Management Guidelines for adult patients with thyroid nodules and differentiated thyroid cancer: the American Thyroid Association Guidelines Task Force on thyroid nodules and differentiated thyroid cancer. Thyroid. 2016;26(1):1–133.
10. Nagarajan N, et al. Conventional smears versus liquid-based preparations for thyroid fine-needle aspirates: a systematic review and meta-analysis. J Am Soc Cytopathol. 2015;4(5):253–60.
11. Cibas ES, Ali SZ. The 2017 Bethesda system for reporting thyroid cytopathology. Thyroid. 2017;27(11):1341–6.
12. Pusztaszeri M. Birefringent crystals in thyroid fine-needle aspiration cytology. Diagn Cytopathol. 2016;44(10):814–5.
13. Layfield LJ, Wax T, Jones C. Cytologic distinction of goiterous nodules from morphologically normal thyroid: analyses of cytomorphologic features. Cancer. 2003;99(4):217–22.
14. Das DK. Marginal vacuoles (fire-flare appearance) in fine needle aspiration smears of thyroid lesions: does it represent diffusing out of thyroid hormones at the base of follicular cells? Diagn Cytopathol. 2006;34(4):277–83.
15. Gupta A, et al. Cytomorphologic significance of marginal vacuoles in diffuse thyroid enlargements. J Cytol. 2013;30(2):125–9.
16. Dufour DR, Wilkerson SY. The normal parathyroid revisited: percentage of stromal fat. Hum Pathol. 1982;13(8):717–21.
17. Obara T, Fujimoto Y, Aiba M. Stromal fat content of the parathyroid gland. Endocrinol Jpn. 1990;37(6):901–5.
18. Roth SI, Capen CC. Ultrastructural and functional correlations of the parathyroid gland. Int Rev Exp Pathol. 1974;13:161–221.
19. Dimashkieh H, Krishnamurthy S. Ultrasound guided fine needle aspiration biopsy of parathyroid gland and lesions. Cytojournal. 2006;3:6.
20. Owens CL, et al. Parathyroid hormone assay in fine-needle aspirate is useful in differentiating inadvertently sampled parathyroid tissue from thyroid lesions. Diagn Cytopathol. 2008;36(4):227–31.
21. Domingo RP, et al. Identification of parathyroid tissue in thyroid fine-needle aspiration: a combined approach using cytology, immunohistochemical, and molecular methods. Diagn Cytopathol. 2017;45(6):526–32.
22. Absher KJ, et al. Parathyroid cytology: avoiding diagnostic pitfalls. Head Neck. 2002;24(2):157–64.
23. Odronic SI, Reynolds JP, Chute DJ. Cytologic features of parathyroid fine-needle aspiration on ThinPrep preparations. Cancer Cytopathol. 2014;122(9):678–84.
24. Park GS, et al. Liquid-based cytology in the fine needle aspiration of parathyroid lesions: a comparison study with the conventional smear, ThinPrep, and SurePath. Int J Clin Exp Pathol. 2015;8(10):12160–8.
25. Chang KJ, Erickson RA, Nguyen P. Endoscopic ultrasound (EUS) and EUS-guided fine-needle aspiration of the left adrenal gland. Gastrointest Endosc. 1996;44(5):568–72.
26. Fassina AS, Borsato S, Fedeli U. Fine needle aspiration cytology (FNAC) of adrenal masses. Cytopathology. 2000;11(5):302–11.
27. Lumachi F, et al. CT-scan, MRI and image-guided FNA cytology of incidental adrenal masses. Eur J Surg Oncol. 2003;29(8):689–92.
28. Jhala NC, et al. Endoscopic ultrasound-guided fine-needle aspiration biopsy of the adrenal glands: analysis of 24 patients. Cancer. 2004;102(5):308–14.
29. Stelow EB, et al. Sampling of the adrenal glands by endoscopic ultrasound-guided fine-needle aspiration. Diagn Cytopathol. 2005;33(1):26–30.
30. Wu HH, et al. Fine needle aspiration cytology of benign adrenal cortical nodules. A comparison of cytologic findings with those of primary and metastatic adrenal malignancies. Acta Cytol. 1998;42(6):1352–8.